Golden Modulation: A New and Effective Waveform for Massive IoT

Lorenzo Vangelista, *Senior Member, IEEE*, Bruno Jechoux, Jean-Xavier Canonici,
and Michele Zorzi, *Fellow, IEEE*

Abstract— **Massive Internet of Things systems, e.g., Low Power Wide Area Networks, aim at connecting very large numbers of low-cost devices with multi-year battery life requirements, a goal that is hard to achieve with current technologies. In this paper, a novel asynchronous spread spectrum technique, called Golden Modulation, is introduced. This modulation provides a vast family of equivalent waveforms with very low cross-correlation even in asynchronous conditions, hence enabling naturally massive multiuser operation without the need for inter-user synchronization or interference cancellation receivers. The basic modulation principles, which rely on spectrum spreading via direct Zadoff-Chu sequences modulation, are presented and the corresponding theoretical bit error rate performance in additive white Gaussian noise and multi-path channels is derived and compared by simulation with realistic receiver performance. The demodulation of the Golden Modulation is described, and its performance in the presence of uncoordinated multiple users is characterized and compared against LoRa in a variety of scenarios. Various higher-layer and backward compatibility issues are also discussed.**

Index Terms— **Massive IoT, low power wide area networks, Zadoff-Chu sequences, asynchronous spread spectrum.**

I. Introduction

MASSIVE access for the Internet of Things (IoT) has been investigated for quite some time (see, e.g., [2]) and is a hot research topic for current and future systems, such as 6G (see, e.g., [3]). Solutions avoiding the need for device coordination (which typically requires significant energy and communications resources) are considered as particularly promising (see, e.g., [4]). For IoT systems operating in the licensed spectrum, of which NB-IoT [5] is currently the most popular solution, research focuses on access schemes,

and the waveform design is based on variations of multi-carrier modulations (see [6] in [7]). Instead, the waveforms used for IoT systems operating in the unlicensed spectrum exhibit a wide variety. Traditional solutions range from the usual Cyclic Prefix-OFDM (Orthogonal Frequency Division Multiplexing) multicarrier modulation for DECT-2020 New Radio [8] to ultra-narrowband D-BPSK (Differential Binary Phase Shift Keying) for the SigFox systems [9]. A new spread spectrum waveform emerged with the LoRa/LoRaWAN® system [10], [11], which gained strong momentum and, at the time of writing, is worldwide the most popular system for massive IoT in unlicensed bands. The wide deployment of LoRaWAN networks highlighted some critical aspects related specifically to situations in which the density of End Devices (EDs) is very high [12], [13]. The ability of LoRa/LoRaWAN to multiplex concurrent data transmissions by different EDs depends on the availability of different "orthogonal" waveforms, also known as logical channels. When the density of EDs becomes high, the number of logical channels may become the bottleneck, causing the network to be congested. The fact that the "orthogonal" waveforms are actually not fully orthogonal (see [14]) makes the problem even worse.

From the above discussion, it emerges that a major open problem in massive access for the Internet of Things (IoT) lies fundamentally in the design of the waveform, which must be such that (i) a very large number of distinguishable channels are available, thereby accommodating a large number of users, and (ii) the cross-correlation between waveforms defining different channels is small, thereby keeping cross-channel interference low. In the LoRa systems, in each frequency channel, separate logical channels are obtained by using different Spreading Factors (defined by the number of transmitted samples per information symbol [10], [11]), whose number is limited to 6 since they can take a value in the set $\{7, 8, \dots, 12\}$ [15]. It must be noted that research for good linear frequency modulated signals, such as those used in LoRa, is still active [16].

In this paper we provide the design and evaluation of a novel set of waveforms, called Golden Modulation (GM), which departs conceptually from linear frequency modulated signals (a characteristic of the LoRa Modulation) and allows a very significant increase in the number of parallel channels, compared to the state of the art mentioned above. This modulation supports flexible bandwidth and spreading factor as well as very good uncoded sensitivity. In addition, it provides a wide family of equivalent waveforms with very low cross-interference, even under asynchronous conditions. More

precisely, GM achieves very low interference between uncoordinated users, hence enabling natural multi-user operation by multiplexing autonomously operating users separated by their waveforms, without the need for inter-user synchronization or for interference cancellation receivers. We remark that LoRa modulation provides only one waveform per spreading factor while hundreds or even thousands of available waveforms (see Table III in Section V) are possible using GM.

GM is based on a novel and generalized perspective on the use of the well-known Zadoff-Chu sequences [17]. This feature is enabled by using the Zadoff-Chu sequences to carry information rather than (as is usually done) for synchronization and/or channel estimation in the headers of a packet in a digital communication link (see, e.g., [18]). In particular, although the use of Zadoff-Chu sequences for signaling was recently discussed in IoT scenarios [19], [20], we are the first to recognize their potential to provide a large number of distinct logical channels and to precisely characterize their interference properties, proposing them as an effective solution for true massive access in the IoT. The efficient implementation of GM is also described in this paper on both the transmitter and receiver sides.

The major contributions of this paper are as follows.

- We provide a novel and generalized perspective on the use of the well-known Zadoff-Chu sequences, recognizing their potential to provide a vast family of waveforms to natively support massive IoT access.
- We design and evaluate a novel set of waveforms, called Golden Modulation (GM), which departs conceptually from linear frequency modulated signals (a characteristic of the LoRa Modulation, the most widely employed system for IoT in the unlicensed spectrum), and allows a very significant increase in the number of logical channels compared to the state of the art.
- We show that, while exhibiting the same error performance as LoRa in the single-user case, GM is able to successfully decode a large number (e.g., a few tens) of parallel asynchronous simultaneous links, whereas current solutions (e.g., those based on the LoRa modulation), can only support one signal at a time (per spreading factor), unless complicated multi-user receivers are used.

The remainder of the paper is organized as follows. In Section II the system requirements for massive IoT systems are reviewed, with emphasis on the effect of network synchronization on the possibility to fulfill the requirements. In Section III, a short description is provided for the frequency-shifted Zadoff-Chu sequences, which are employed in GM. In Sections IV and V, the use of GM is presented in a single-user and multi-user perspective, respectively, along with related results. In Section VI, we provide a preliminary discussion on higher-layer, architectural, and backward compatibility issues. Finally, conclusions are drawn in Section VII.

Notation: For the sake of readability, Table I provides a reference summary of our notation. We refer the reader to [21] for a paper on LoRaWAN using the proposed notation.

II. MASSIVE IoT SYSTEM REQUIREMENTS

Massive IoT aims to connect vast numbers of uncoordinated low-cost devices with multi-year battery life requirements.

TABLE I
A SUMMARY OF THE NOTATION

symbols	explanation
T_c	basic temporal interval between two samples of a digital signal (chip)
$T = N \cdot T_c$	"block" interval of N basic temporal intervals (symbol)
$x(\ell T + kT_c)$	signal at the index $\ell \cdot N + k$
$x_d(k)$	sequence at the index k
$x(t), t \in \mathbb{R}$ $x(t) \in \mathbb{R}$ or $x(t) \in \mathbb{C}$	A generic signal in the continuous-time domain
$x_d(nT_c) \, n \in \mathbb{Z}$ $x_d(nT_c) \in \mathbb{R}$ or $x(t) \in \mathbb{C}$	A generic signal in the discrete-time domain

To achieve such stringent demands, some key bottlenecks must be removed. In particular, the system capacity shortage faced in current LPWANs (Low Power Wide Area Networks), in both unlicensed and licensed spectrum, must be solved. An overall capacity several orders of magnitude higher than what is available in current state-of-the-art LPWANs is required in order to enable the expected number of connections per IoT gateway. This requirement is exacerbated by the emerging paradigm of Direct Device to Satellite communication for LPWANs, where the area covered by a single gateway may be very large [22], [23].

In addition, the device's power consumption must be minimized to enable multi-year battery life. The power consumption of the device is driven on the one hand by the required transmit power and on the other hand by the energy required to synchronize the device with the network. The required degree of network synchronization varies drastically depending on the physical layer and associated link layer of the system: OFDM-based systems such as NB-IoT, LTE catM or the recently introduced DECT 2020 NR require stringent time and frequency synchronization among all devices, coupled with strict resource request and assignment mechanisms in order to maintain orthogonality of the PHY signals and to avoid packet collisions. This has a significant impact in terms not only of energy consumption but also of protocol overhead, since specific channels for downlink synchronization, resource request, and resource grant are then required, and consume radio resources and energy for transmission. In contrast, non-cellular LPWAN systems such as LoRa or SigFox can operate with virtually no network synchronization. It is interesting to note that, due to the characteristics of massive IoT traffic, where each device transmits infrequently small amounts of data, the energy and transmission resources needed for network synchronization and signaling may become dominant over those required to effectively transmit data packets. This is especially true for cellular-based systems such as NB-IoT (also known as 5G IoT) or LTE catM, where the device is managed by the network, which fully controls the access to the medium, implying high power consumption and high control overhead, hence reducing the effective capacity of the system. A comparison between LoRaWAN and NB-IoT has been made in [24], showing that LoRaWAN and NB-IoT have similar performance in terms of network capacity, with

NB-IoT slightly outperforming LoRaWAN for small cells, at the cost of significantly higher energy consumption even without considering the energy cost of network synchronization. The impact of NB-IoT synchronization on the energy budget for each transmission of NB-IoT uplink data packet under real conditions has been analyzed in [25]. Overall, it seems reasonable to state that a scalable massive IoT system must avoid device network synchronization to make device operation as autonomous as possible. It is hence of crucial importance to have a PHY layer able to operate with minimum or no device synchronization requirements while ensuring in addition high sensitivity and high capacity.

The other key requirement for a massive IoT system is its ability to support (and distinguish) many different users. This translates into two different requirements, i.e., (i) the availability of a large number of logically separable channels (which has to do with how the waveform is designed), and (ii) the ability to correctly receive the intended signal when a number of signals are transmitted simultaneously (which has to do with the cross-interference properties of the waveforms).[1] As already mentioned, LoRa (the standard reference in unlicensed LPWANs), does poorly in both respects, as it provides a single waveform per SF (six waveforms in total), with no hard guarantees about cross-interference properties. In this paper, we propose an alternative solution, called Golden Modulation (GM), based on the use of the Zadoff-Chu sequences, whose main properties are that (i) many distinct and distinguishable waveforms are available, so that different users in the system can be assigned different waveforms, and (ii) interfering users can be successfully decoded, provided that the number of simultaneous transmissions is not too large. Based on these properties, GM is able to truly unlock the capacity bottleneck of massive IoT systems.

III. THE FREQUENCY SHIFTED ZADOFF-CHU SEQUENCES

According to [17], we can express the frequency shifted Zadoff-Chu Sequences as follows

$$Z_N^{r,q}(k) = \begin{cases} e^{j\frac{\pi}{N}r(k+1+2q)k} & \text{for } N \text{ odd} \\ e^{j\frac{\pi}{N}r(k+2q)k} & \text{for } N \text{ even} \end{cases} \quad (1)$$

where $q \in \mathbb{Z}$, $N \in \mathbb{N}, N \neq 0$, $r \in \mathbb{N}$, $\gcd(r,N) = 1$, and $k = 0, \ldots, N-1$. Usually, r is called the "root" of the sequence, N its "length," and q its "offset." It must be noted that, although in general $q \in \mathbb{Z}$, meaningful values are in the set $\{0, 1, \ldots, N-1\}$. For example, when $q \geq N$, Equation (1) becomes

$$Z_N^{r,q}(k)$$
$$= \begin{cases} e^{j\frac{\pi}{N}r(k+1+2q)k} = e^{j\frac{\pi}{N}r(k+1+2(q\,\text{mod}N))k} & \text{for } N \text{ odd} \\ e^{j\frac{\pi}{N}r(k+2q)k} = e^{j\frac{\pi}{N}r(k+2(q\,\text{mod}N))k} & \text{for } N \text{ even} \end{cases}$$
$$(2)$$

where clearly $(q \bmod N) \in \{0, 1, \ldots, N-1\}$. Similarly, we will assume that $r \in \{1, \ldots, N-1\}$.

From Equations (9) and (10) in [17], we have that the cyclic autocorrelation of the sequence $Z_N^{r,q}(\cdot)$ is non-zero only for a shift equal to 0. From [26], we have that by selecting N odd and any pair of roots $r_1 \neq r_2$ such that $\gcd(r_1 - r_2, N) = 1$, the cyclic cross-correlation between the two Zadoff-Chu sequences $Z_N^{r_1,q}(\cdot)$ and $Z_N^{r_2,q}(\cdot)$ is equal to $\frac{1}{\sqrt{N}}$. In particular, if N is a prime number, $(r_1 - r_2)$ is always relatively prime to N, whichever the selected pair of roots (r_1,r_2),[2]

IV. THE GOLDEN MODULATION: SINGLE LINK DESCRIPTION AND PERFORMANCE ANALYSIS

Suppose we have a source of M-ary symbols $M < N$ (see Section III and Equation (2)), emitting symbols at rate R. We indicate the generic symbol in the symbol period ℓT as $q(\ell T) = q_\ell \in \{0, 1, \ldots, M-1\}$, $T = 1/R$, $\ell \in \mathbb{N}$, and denote the "chip" period as $T_c = T/N$. Then, the discrete-time modulated GM signal in the symbol period ℓT is

$$x(\ell T + kT_c) \stackrel{\text{def}}{=} Z_N^{r,q_\ell}(\ell N + k) , \quad k = 0, \ldots, N-1 \quad (3)$$

where the ℓ-th information symbol q_ℓ is mapped to a length-N Zadoff-Chu sequence with offset q_ℓ.

In order to obtain an expression of the modulated signal highlighting its dependence on the set $\{q_\ell, N, r\}$ that define the parameters and the symbol, we rewrite Eq. (3), providing an alternative expression for the modulated signal, as

$$x(\ell T + kT_c; q_\ell, N; r) \stackrel{\text{def}}{=} Z_N^{r,q_\ell}(\ell N + k). \quad (4)$$

For a generic time nT_c, defining $\ell(n) \stackrel{\text{def}}{=} \lfloor \frac{n}{N} \rfloor$ and $k(n) \stackrel{\text{def}}{=} n \bmod N$, we can write the discrete time modulated signal as

$$x_d(nT_c; q_\ell, N; r) = x(\ell(n)T + k(n)T_c; q_{\ell(n)}, N; r). \quad (5)$$

These alternative expressions for the modulated signals will be needed in the following, depending on the context, for example to assess the orthogonality or in Section V.

As in [11], we set $T_c = \frac{1}{B}$, where B is the bandwidth occupied by a GM link. As a consequence, the symbol duration is $T = \frac{N}{B}$, so that the symbol rate is $R = \frac{B}{N}$ and the bit rate $R_b = b \cdot \frac{B}{N}, b = \log_2 M$. For a given sequence length N, we can define by analogy the Spreading Factor for GM as[3]

$$SF \stackrel{\text{def}}{=} \log_2 N . \quad (6)$$

GM demodulation is based on the orthogonality of Zadoff-Chu sequences with the same root and offsets q, q'. We have that

$$\frac{1}{N} \sum_{k=0}^{N-1} x(\ell T + kT_c; q, N; r) \cdot x^*(\ell T + kT_c; q', N; r)$$
$$= \begin{cases} 1 & q = q' \\ 0 & q \neq q' \end{cases} \quad (7)$$

so the discrete-time signal space for the GM modulation admits as an orthonormal basis the set of sequences $\frac{1}{\sqrt{N}}x(kT_c; q, N; r)$ indexed by the possible transmitted symbol

---

[1]We remark that the two requirements are different, as having a very large number of logical channels does not necessarily mean that many of them are used simultaneously.

[2]Since $r_1 < N$ and $r_2 < N$, when $(r_1 - r_2) < 0$ we will take $(r_1 - r_2)$ to be equivalent to $(N + (r_1 - r_2))$.

[3]Note that, unlike in LoRa, the sequence length does not need to be a power of 2. The issue of how to select N will be discussed later in the paper.
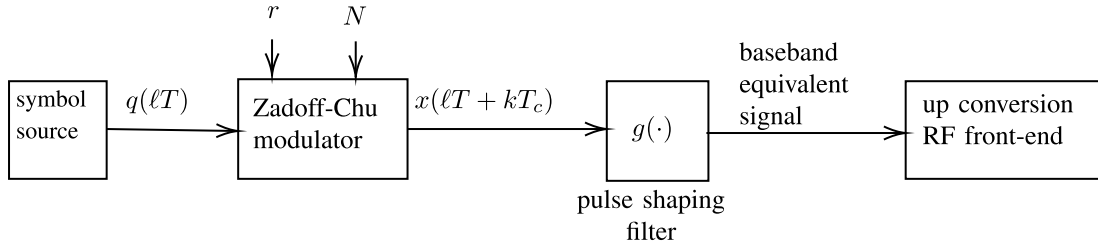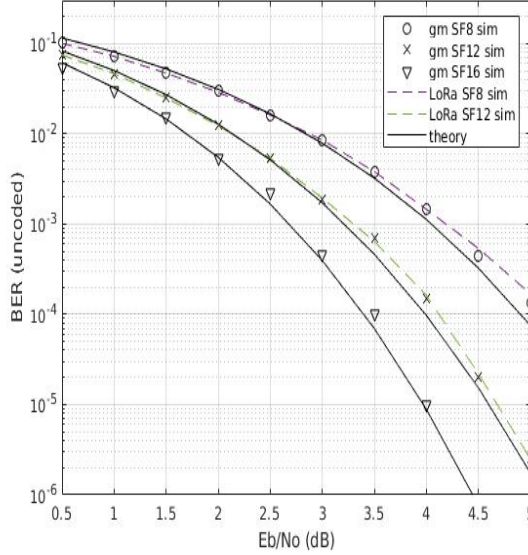
Fig. 1. The golden modulator.

Fig. 2. Theoretical approximation and simulated BER of the golden modulation for $SF = 8, 12, 16$, and of LoRa for $SF = 8, 12$.

$q \in \{0, 1, \ldots, M - 1\}$ and for the running time index $k \in \{0, 1, \ldots, N - 1\}$. We then observe that we are in the same conditions as in [27]. By re-using the same arguments and the proof as in [27], Sections II and III-A, the BER performance of GM in an Additive White Gaussian Channel (AWGN) can be accurately approximated by (see the Appendix for details)

$$P_b \approx 0.5\, Q\left(\sqrt{\Gamma\, 2^{SF+1}} - \sqrt{1.386\, SF + 1.154}\right) \quad (8)$$

where Γ is the Signal-to-Noise Ratio (SNR) and $Q(x) = \int_x^\infty \frac{e^{-a^2/2}\, da}{\sqrt{2\pi}}$ is the complementary Gaussian distribution function.

To be transmitted, the discrete-time GM signals must be converted in the continuous time domain through a pulse shaping filter $g(t)$. The complete chain to produce the analog continuous time GM modulated signal is shown in Fig. 1.

A practical choice for the pulse shaping filter $g(t)$ typically results in a signal bandwidth $B_{ch} > \frac{1}{T_c}$. For example, for the widely used root raised cosine waveform, we have $B_{ch} = (1 + \beta)B$, where β is the roll-off factor and determines the excess bandwidth.

We first study the performance of the Golden Modulation in an AWGN channel, which is the usual model considered for terrestrial LPWANs, where a strong dominant Line-of-Sight component is typically present (see, e.g., [28], [29], [30]). This model is even more accurate for Direct Device to Satellite communication, which is a key emerging use case for GM and for massive IoT [22], [23]. The corresponding performance

TABLE II
FIXED 4 TAPS TDL MULTIPATH CHANNEL

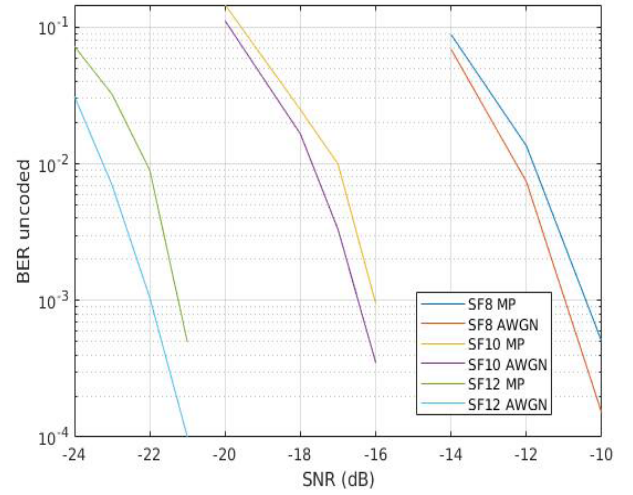| Excess tap delay [ns]	Relative power [dB]
0	0
500	-2
8000	-9
16000	-12

Fig. 3. Bit Error Rate (BER) for the Golden Modulation for an AWGN and the multipath channel of Table II, labeled as MP.

of GM is provided in Fig. 2 for the case of ideal Nyquist filtering, where the uncoded Bit Error Rate (BER) obtained via computer simulations is compared to that obtained via the analytical approximation of Equation (8). Simulation results performed for Golden Modulation with SF 8, 12 and 16 show a very good match with the analytical curves, as expected. The figure also includes the performance of LoRa (only for SF 8 and 12, as in LoRa SF 16 is not available), showing that it is essentially the same as that of GM,

For completeness, we also evaluated the performance of the Golden Modulation in a multi-path scenario, using a multipath channel whose specification, reported in Table II, is a Tapped Delay Line (TDL) with 4 taps. The results are shown in Fig. 3.

To conclude the characterization of the Golden Modulation, in Fig. 4 the Power Spectral Density for a bandwidth of 125 kHz and $SF = 7$ ($N = 128$) is shown.[4] As in [11], the figure also reports the ETSI masks from [31], showing that the bandwidth occupancy of GM is the same as in LoRa.

---

[4]We remark that this result is general, as the power spectral density is independent of the spreading factor.
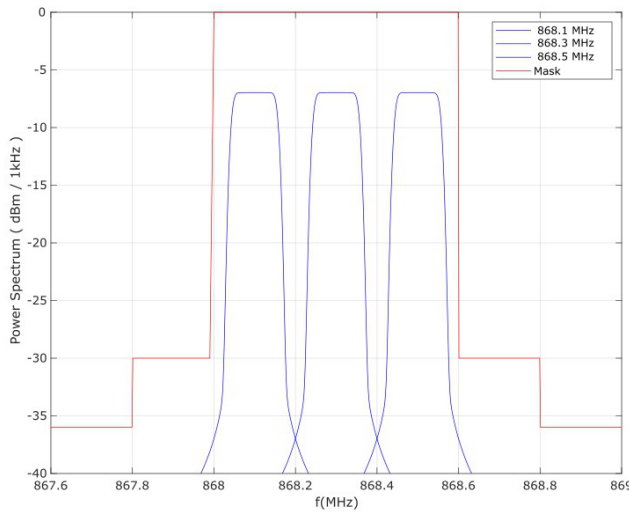
Fig. 4.   Power spectral density of 3 GM channels with a bandwidth of 125 kHz (centered at 868.1, 868.3 and 868.5 MHz) and $SF = 7$ compared to the ETSI mask from [31].

A. *The Receiver - Single Link*

Ignoring for the sake of simplicity the effect of the transmission channel and assuming N odd, to demodulate the symbol transmitted in the period ℓT we consider the received signal

$$y(\ell T + kT_c) \overset{\text{def}}{=} e^{\jmath \frac{\pi}{N} r(k+1+2q_\ell)k} + w(\ell T + kT_c) \qquad (9)$$

$k = 0, \ldots, N - 1$, where $w(\cdot)$ is a Complex Additive White Gaussian Noise ($\mathcal{C}$AWGN), with variance σ_w^2. Since the receiver is assumed to know the parameters r and N,[5] it can compute the signal

$$y_m(\ell T + kT_c) \overset{\text{def}}{=} \left[e^{\jmath \frac{\pi}{N} r(k+1+2q_\ell)k} + w(\ell T + kT_c) \right] \cdot$$
$$\cdot e^{-\jmath \frac{\pi}{N} r(k+1)k}$$
$$= e^{\jmath \frac{2\pi}{N} q_\ell k} + w_m(\ell T + kT_c) \qquad (10)$$

where $w_m(\ell T + kT_c) \overset{\text{def}}{=} w(\ell T + kT_c) \cdot e^{-\jmath \frac{\pi}{N} r(k+1)k}$ is also $\mathcal{C}$AWGN with variance σ_w^2.

Now the problem reduces to estimating the frequency (i.e., the symbol q_ℓ) of a single tone in $\mathcal{C}$AWGN. As shown in [10], this problem can simply be solved via a DFT. In particular, the value of q_ℓ can be obtained by forming the N dimensional vector

$$\mathbf{Y}(\ell T) = \begin{bmatrix} y_m(\ell T + 0 \cdot T_c) \\ y_m(\ell T + 1 \cdot T_c) \\ \vdots \\ y_m(\ell T + (N-1) \cdot T_c) \end{bmatrix}, \qquad (11)$$

computing $\mathbf{Z}(\ell T) = \text{DFT}(\mathbf{Y}(\ell T))$, and taking the index of the entry with largest magnitude. Having found the index i, the estimated symbol is $q_\ell = i$. In particular, if N is prime, the DFT can still be made with a complexity similar to the usual radix–2 one via the FFTW algorithm [32]. This complexity is the same as in LoRa systems.

We can summarize the single link characteristics of GM as follows:

---

[5]For example, these values could have been negotiated with the network server when the node joined the network.

- Zadoff-Chu sequences with given length N and root r can be successfully used to carry information modulated in the offset q, which can be easily extracted at the receiver using a simple DFT, with the same complexity as in LoRa.
- The BER performance of GM can be closely approximated by the analytical expression in (8), and is therefore equivalent to that of LoRa.
- The spectrum occupancy of GM signals meets the ETSI mask requirements, and is equivalent to that of LoRa.

Therefore, from the point of view of a single link, GM and LoRa exhibit very similar behaviors, and can be considered as equivalent. Actually, as stated in [20], "The FSCM modulation employed in the LoRa signalling scheme is an orthogonal modulation with symbols encoded using a set of N cyclically shifted versions of a base Zadoff-Chu (ZC) sequence." As we will discuss in the next section, the situation is very different in the multi-user case, where GM can be shown to have vastly superior performance than LoRa in terms of interference mitigation and multi-user capacity. Finally, even though the GM modulation could be seen as a DSSS CDMA (Direct Sequence Spread Spectrum Code Division Multiple Access) scheme, DSSS CDMA systems based on generic pseudo random sequences are not suitable for massive IoT since, for example, they require system synchronization. For this reason, a direct comparison of GM with DSSS CDMA systems is not meaningful here.

V. THE GOLDEN MODULATION: MULTIPLE LINK DESCRIPTION AND PERFORMANCE ANALYSIS

In this section, we consider the superposition of multiple signals on the same channel in GM, and show how the properties of the Zadoff-Chu sequences can be used to successfully decode most of them. As discussed in Section IV, a Zadoff-Chu sequence is defined by the following parameters: the offset q (which in GM is used to carry the information symbol), and the length N and the root r, which can be used to define "quasi-orthogonal" logical links.

Recall that, in LoRa, only one waveform per spreading factor is available, which limits to 6 the number of logical links available. Therefore, the multiple access scheme used in LoRaWAN is essentially an ALOHA protocol for each SF, and multiple users transmitting simultaneously using the same SF will collide and be undecodable (unless complex multi-user receivers are implemented).

To study the multi-user performance of GM, consider first the case in which the sequence length N and the alphabet size M are fixed. We know from Section III that, by selecting N odd and any pair of distinct roots $r_1 \neq r_2$ such that $\gcd(r_1 - r_2, N) = 1$ (which is always true if N itself is prime), the signals in the time interval $\{\ell T, \ell T + T_c, \ldots, \ell T + (N-1)T_c\}$, namely $x(\ell T + kT_c; q_\ell^{(1)}, N; r_1)$ and $x(\ell T + kT_c; q_\ell^{(2)}; N; r_2)$, have their cyclic cross-correlation constant and equal to $\frac{1}{\sqrt{N}}$, for any choice of the transmitted symbols $q_\ell^{(1)}, q_\ell^{(2)}$.

In general, given N prime, a set of $K \leq N - 1$ distinct roots $\mathcal{R}_{N,K} = \{r_1, r_2, \ldots r_K\}$ can be selected such that $\gcd(r_i - r_j, N) = 1$ for $r_i, r_j \in \mathcal{R}_{N,K}, i \neq j$. Any link such
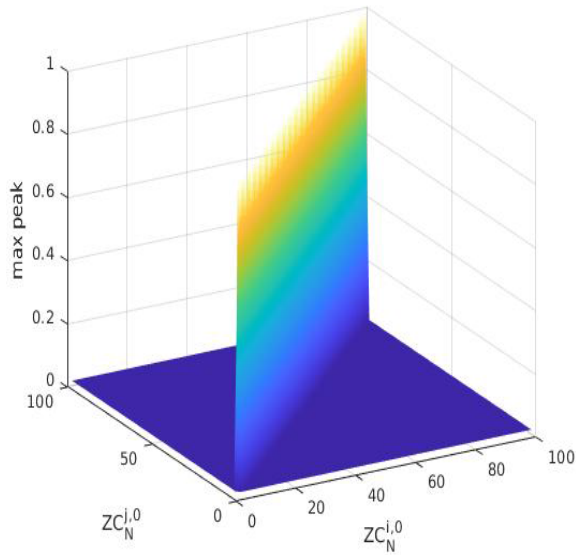
Fig. 5. Cyclic cross-correlation maximum peaks for $N = 2053$ Zadoff-Chu sequences $Z_N^{r_i,0}(k)$ and $Z_N^{r_j,0}(k)$ (subset of 100 roots); indices i and j are plotted on the two horizontal axes.

as the one described in Section IV, using the root $r_i \in \mathcal{R}_{N,K}$, is then "almost" orthogonal to any other link of the same type using a different root $r_j \in \mathcal{R}_{N,K}$, $i \neq j$. More precisely, the signals $x_d(nT_c; q_\ell^{(i)}, N; r_i)$ and $x_d(nT_c; q_\ell^{(j)}, N; r_j)$ have a low (equal to $\frac{1}{\sqrt{N}}$) cyclic cross-correlation and the symbols $q_\ell^{(i)}$ and $q_\ell^{(j)}$ transmitted by the two links can be recovered using two parallel and independent DFT receivers as described in Section IV-A. The only difference is that, besides noise, now there is also interference, but the cross-correlation properties of the Zadoff-Chu sequences with different roots guarantee that the *pairwise* Signal to Interference Ratio is proportional to $\sqrt{N}$, so that, for sufficiently large N, multiple interferers can be tolerated. Therefore, a number of users proportional to $\sqrt{N}$ can be supported.

The above performance applies identically to the full set of Zadoff-Chu sequences of length N as illustrated in Fig. 5, which shows the cross-correlation results between any two sequences from a set of 100 Zadoff-Chu sequences of length 2053. The set of "quasi orthogonal" Golden Modulation signals that can be assigned to EDs is hence very large (up to $N - 1$) and increases with the spreading factor. Similarly, the orthogonality level between users increases with the spreading factor as shown in Table III, where "interference rejection" is the highest value of the cross-correlation between a symbol with a certain SF and any other symbol with the same SF.[6]

A remark on Figure 5 is in order. As expected, when the two sequences are the same, i.e., $i = j$, we observe a large peak equal to 1. In all other cases (i.e., $i \neq j$) the maximum peak is much smaller (with a value of $1/\sqrt{N} \simeq 0.022$) and independent of i and j (i.e., it is flat, as can be observed from Figure 5).

---

[6]For each Spreading Factor SF, N was chosen as the smallest prime number greater than or equal to 2^{SF}. It is also possible to truncate such a sequence to a length exactly equal to 2^{SF}, for compatibility with existing systems, as discussed in Section VI.

TABLE III
NUMBER OF GOLDEN MODULATION WAVEFORMS AND INTERFERENCE LEVELS PER SF

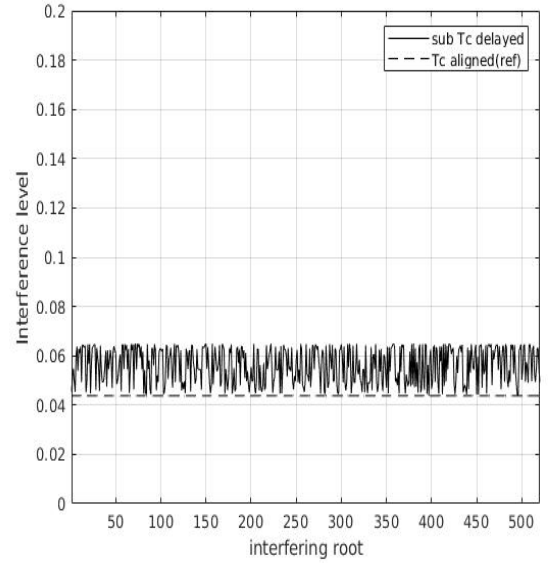| Spreading SF	Interference Rejection dB	Waveforms Set Size $N - 1$
7	-10.6	130
8	-12.0	256
9	-13.6	520
10	-15.1	1030
11	-16.6	2052
12	-18.1	4098
13	-19.6	8208
14	-21.1	16410
15	-22.6	32770
16	-24.1	65536

Fig. 6. Crosscorrelation maxima between symbols of an $SF = 9$ link and any uncoordinated (not time aligned) interfering link with $SF = 9$ and a different root.

It must be noted that comparable performance can be obtained when considering two "uncoordinated" links, i.e., links that are not aligned in time. In this case, since signals issued by different users reach the receiver with independent timing, the underlying Zadoff-Chu sequences of the different links overlap asynchronously, and interference will appear at the correlator output, depending on their aperiodic cross-correlation. The correlation properties of polyphase sequences have been extensively studied in the literature, see, e.g., [33], [34], [35], [36], and [37] eventually derived the aperiodic cross-correlation bounds for Zadoff-Chu sequences. These bounds show the very good aperiodic correlation properties of Zadoff-Chu sequences, as illustrated in the example of Fig. 6, which plots the maximum interference level experienced by a target link with $SF = 9$ due to all possible other uncoordinated interfering signals with $SF = 9$.

Fig. 7 shows the interference level between different GM signals with the same SF, as a function of the time shift, showing that the maximum interference level is almost independent of the time delay. In particular, to study the effect of fractional misalignment between the two sequences, we plotted the cross-correlation values for all time-shifts that are multiples of $T_c/4$. While for time-shifts multiples of T_c the normalized
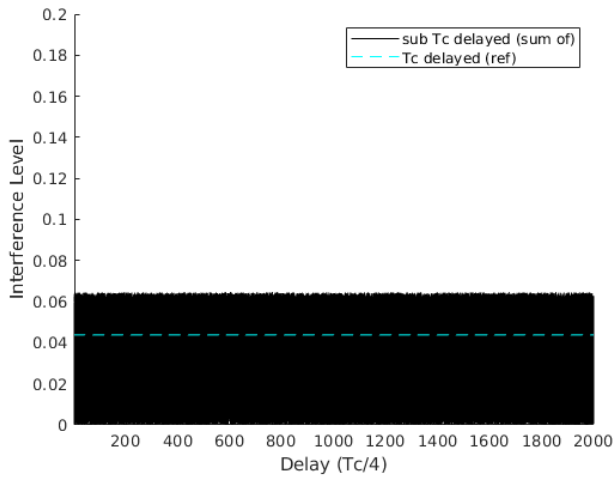
Fig. 7. Crosscorrelation between symbols of uncoordinated $SF = 9$ links depending on delays (100 randomly selected interferers with random sub Tc delays).

Fig. 8. Impact of multiuser interference on GM demodulation for $SF = 8, 10, 12$ and 14.

interference level is $1/\sqrt{N}$ ($\simeq 0.0438$ for $N = 521$ in this case, represented by the horizontal dashed line), for fractional time-shifts the possible values of the interference level vary within the range from 0 to about 0.065, showing that fractional misalignment has a modest price in terms of a (uniformly bounded) interference increase (about 2 dB in the worst case).

Golden Modulation leverages these low cross-correlation properties of the filtered Zadoff-Chu sequences to provide ultra-high capacity without any penalty in terms of range or power consumption. This is a major advantage from a system point of view since multiple devices can transmit simultaneously using different Zadoff-Chu roots without the need for any synchronization between the different transmissions, hence avoiding the need for complex and energy consuming synchronization mechanisms. This enables an increase of the system capacity of IoT networks by several orders of magnitude, without paying any penalty in terms of single link performance, power consumption, and receiver complexity.

The performance of GM in a multi user configuration is presented for $SF = 8, 10, 12$ and 14 in Fig. 8, where packets from the different users are received with equal power and random delays. It can be seen that the demodulation performance of Golden Modulation remains very good in the presence of several tens of simultaneous interfering devices while LoRa is limited to the reception of a single packet per SF (provided that it is free of collisions). More specifically, the number of packets that can be simultaneously supported depends on the BER target and on the value of SF (sequence length N): for example, for a BER target of 0.01, GM is able to support from about 20 simultaneous transmissions at $SF = 8$ up to more than 100 for $SF = 14$.

The high-capacity multi-access performance of GM can therefore be summarized as follows:

- The availability of up to $N - 1$ pairwise quasi-orthogonal Zadoff-Chu sequences makes it possible to assign different sequences to different users, thereby creating up to $N - 1$ separable logical channels.
- Any choice of a limited number of users who transmit simultaneously can potentially lead to the correct
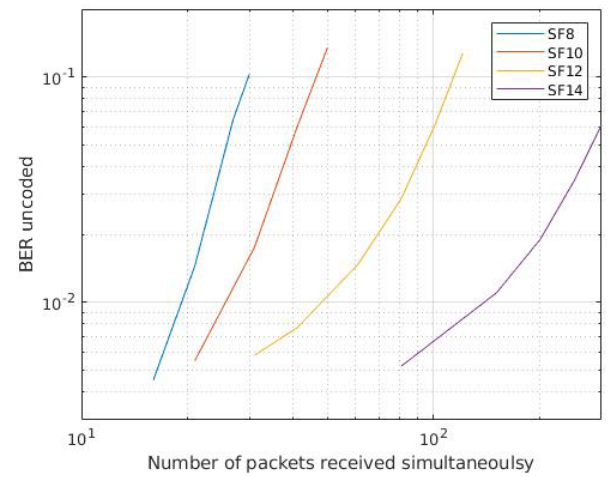
decoding of all of them thanks to the interference rejection capabilities provided by the cross-correlation properties of Zadoff-Chu sequences.

A simplified view of this behavior, which applies precisely in an AWGN scenario where signals are received with the same power, corresponds to an ALOHA system with multi-packet reception capabilities [38], in which the receiver is able to correctly decode all received signals as long as their number is below a certain threshold, whereas in the presence of too many signals all packets are lost (collision). We remark that the threshold on the number of packets that can be simultaneously received in GM increases for larger N (i.e., for higher spreading factors), whereas in LoRaWAN this threshold is equal to 1 (simultaneous transmissions with the same SF always lead to a collision).

A. Multiple Users With Different Spreading Factors

The above treatment of the multi-access performance of GM assumed a fixed sequence length N, shared by all users. We remark that, in practical situations, this may not be the case, as EDs in an LPWAN autonomously trigger their transmissions at rates as dictated by their respective link budget and their respective application. In this subsection, we consider the case where two EDs may use two generic lengths N_1 and N_2 (i.e., spreading factors), not necessarily equal, using roots $r_i \in \mathcal{R}_{N_1, K_1}$ and $r_j \in \mathcal{R}_{N_2, K_2}$. The generic two users may (and usually will) also be uncoordinated, i.e., not aligned in time.

Golden Modulation, relying on the properties of its underlying Zadoff-Chu sequences, exhibits a "quasi-orthogonality" between signals with different Spreading Factors as well, whichever their roots. As an example, the interference generated by a signal with different Spreading Factor (i.e., different N) is shown in Fig. 9, which plots the output of the receiver that results from the superposition of an intended signal and an uncoordinated interferer operating with $SF = 11$ and $SF = 10$, respectively. The intended signal produces the expected peak of value $N = 2053$ at the output of the correlator according to its time-shift (around 1000 samples in this case) and zero autocorrelation otherwise, whereas the
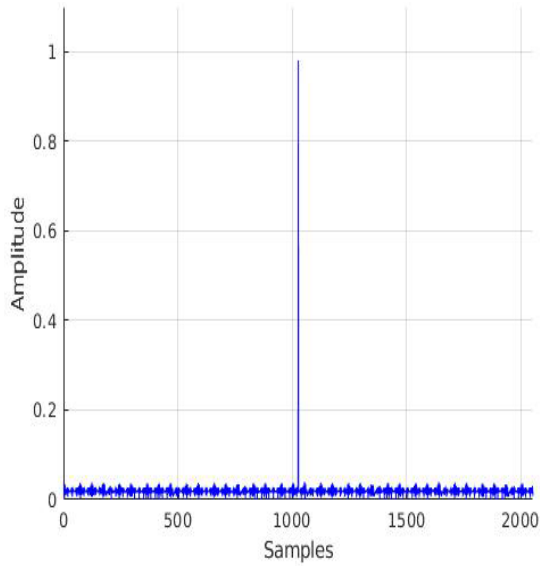
Fig. 9. Correlator output for an $SF = 11$ link in the presence of an uncoordinated interfering link with $SF = 10$.

interferer produces low cross-correlation values for all possible time-shifts, confirming the good cross-correlation properties of these waveforms even for different spreading factors.

VI. GOLDEN MODULATION NETWORKS: HIGHER-LAYER PROTOCOLS AND NETWORKING

While the main focus of this paper is on the new waveforms used in the Golden Modulation and on their transmission performance and cross-correlation properties, in this section we briefly address a number of issues at the system level, including general receiver structure, architecture, higher-layer protocols, and backward compatibility with existing systems.

A. The General Receiver

The Golden Modulation frame is made of a series of concatenated Zadoff-Chu sequences covering a preamble and a payload section (see the frame format in Fig. 10). Frames issued by different devices can advantageously use different roots, which allows easy multiuser reception without the need for device coordination. It must be highlighted that there are $N - 1$ possible roots for Zadoff-Chu sequences of length N, hence providing the potential for the generation of thousands of "quasi orthogonal" frames with the same or different SF, totally unlocking the IoT networks capacity. In addition, the ability to support the highly desirable uncoordinated mode of operation guarantees robustness and extremely low protocol overhead.

The results in Section V show that a correlator that uses the sequence assigned to a given user with root r_i is able to attenuate the interference caused by other users using different roots, $r_j \neq r_i$. Therefore, multiple simultaneous signals sent by different users to a gateway can be successfully received by implementing a number of parallel such receivers, each tuned to a certain user by selecting the corresponding

sequence length (N) and root (r).[7] As long as the total number of overlapping signals is within the interference suppression capabilities of the used sequences (as per the results shown in Fig. 8), all signals can be decoded correctly by the parallel receivers, without any need for complex interference cancellation or multi-user detection, as interference is nativey handled thanks to the properties of the Zadoff-Chu sequences.

More specifically, the general parallel receiver at the gateway must be able to search for all sequences that exist in the system (i.e., that have been assigned to the users), so as to determine which signals are actually present and to synchronize on each of them. The general packet consists of a PHY preamble and a PHY payload (which is the layer-2 frame), see Fig. 10. The preamble, used for packet detection and synchronization, is just the repetition of a predefined symbol, q_0, a certain number of times (e.g., 8), and is modulated using the ZC sequence with length and root that correspond to a certain user.[8] The payload is also modulated using the same sequences, except that in this case the payload content corresponds to a sequence of symbols (i.e., offsets) instead of the predefined q_0.

This architecture is similar to the receiver implemented in LoRa chips where, typically, there are 8 programmable fingers, "launched" by the receiver to detect packets with possible different spreading factors. In the GM case, the set of single-user receivers works very well due to the good pseudo-orthogonality of the sequences. This is not the case instead for LoRa modulation, as the pseudo-orthogonality of the transmission with different lengths $N = 2^{SF}$ (SF being the spreading factor) is not precisely characterized [14]. LoRaWAN multi-user receivers have been investigated (see [39], for example), but the number of overlapping packets that can reasonably be decoded by a LoRa multi-user receiver is limited to very few, while in GM multiple single-user independent receivers can successfully decode several tens of interfering packets (see Fig. 8).

Regarding the complexity issue, we remark that although the GM receiver is complex (if we want to exploit its full potential we may need thousands of instances of the single-user receiver), it is intrinsically parallel and, as a consequence, can be efficiently implemented in parallel machines such as those used for machine learning tasks, e.g., GPUs, which are the de-facto standard and highly optimized for parallel tasks.

B. A Possible Architecture of an LPWAN Based on GM

In this subsection we briefly describe a possible network architecture for an LPWAN based on GM.

The architecture is made of 3 functional entities, namely, the *End Device (ED)*, the *gateway*, and the *back-end*. Each ED will send and receive packets to/from the gateway, according to the application being supported. These packets will have the format described in Fig. 10 and will be sent using GM

---

[7]The parameters of each user can be exchanged during the join procedure, in which the network server can assign a unique pair of sequence length and root to an incoming user.

[8]This assumption is inspired by the signaling procedures of LoRaWAN. Following the same approach as LoRaWAN, the symbol q_0 and the length of the preamble can be fixed at the system level.

FRAME

PREAMBLE | PAYLOAD

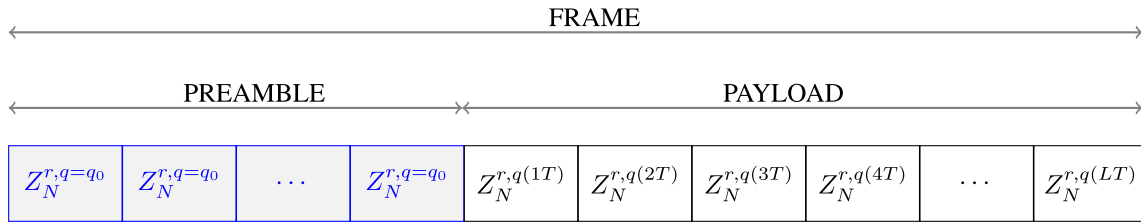| $Z_N^{r,q=q_0}$ | $Z_N^{r,q=q_0}$ | $\cdots$ | $Z_N^{r,q=q_0}$ | $Z_N^{r,q(1T)}$ | $Z_N^{r,q(2T)}$ | $Z_N^{r,q(3T)}$ | $Z_N^{r,q(4T)}$ | $\cdots$ | $Z_N^{r,q(LT)}$ |

Fig. 10.   Example of golden modulation frame format.

as the physical layer technology (the focus of this paper). The gateway will receive and decode these packets (as well as also possibly sending downlink packets, according to the application), and forward them to the back-end using wired or wireless connectivity, typically based on the IP protocol. In particular, in the back-end will reside applications typical of LPWANs, for example metering of gas, water and electricity.

In typical LPWAN settings, the network may include a very large number of EDs, multiple gateways, and a back-end. Therefore, there are multiple links, possibly with different data rates, between each gateway and the EDs in its coverage area. In addition, in LPWANs (and in LoRaWAN in particular), the activation of any node is random and therefore packet transmissions are not synchronized across the network. While in LoRaWAN this may result in collisions and in the consequent loss of all packets involved, GM can handle the situations of multiple simultaneous packet transmissions much more effectively, thanks to the cross-correlation properties of the Zadoff-Chu sequences and according to the spreading factor (i.e., the sequence length), as explained in Section V.

C. Truncated Sequences and Backward Compatibility

It must be noticed that, despite its baseline design using odd-length Zadoff-Chu sequences, Golden Modulation can also be implemented based on even-length sequences. For example, an implementation based on truncated odd length Zadoff-Chu sequences leading to an effective sequence length equal to a power of 2 is also possible. As shown in Fig. 11 (which reports the same results of Fig. 5, except that the sequences have been truncated from $N = 2053$ to $N = 2048$), the degradation of GM's orthogonality is marginal and has no noticeable effect on its performance (for $i \neq j$ the maximum peak is small and almost independent of the indices of the two sequences).

An implementation based on truncated odd-length Zadoff-Chu sequences leading to an effective sequence length equal to a power of 2 is interesting for cases where adaptation to processing units or to size-constrained lower layer protocols is required. The latter case is actually very much of practical use. For example, it is straightforward to implement the LoRaWAN protocols on top of GM with Zadoff-Chu truncated sequences to achieve an effective sequence length equal to a power of 2: once the value of the SF for LoRaWAN is selected, the same SF can be selected for GM. Moreover, once a certain bandwidth B is selected for the LoRaWAN protocol, the same bandwidth B can be selected for GM. All of the specifications (for example [15]) refer to bytes for the fields of any message and the messages can then be immediately translated in bytes carried by GM. As one can notice from Figure 10, the
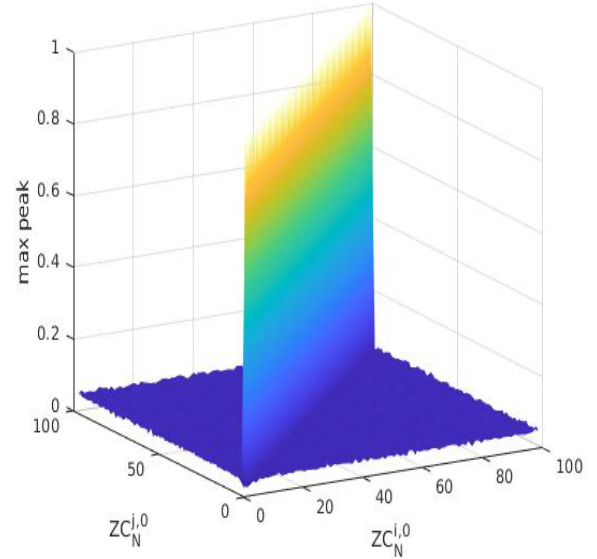

Fig. 11.   Cyclic cross-correlation maximum peaks for the $N = 2053$ Zadoff-Chu sequences $Z_N^{r_i,0}(k)$ and $Z_N^{r_j,0}(k)$ truncated to $N = 2048$ (subset of 100 roots); indices i and j are plotted on the two horizontal axes.

structure (preamble followed by data) is the same. All the "regional parameters" as per [40] are automatically reusable (for the same bandwidth B), ensuring compliance with the regulations worldwide. In general, the complete LoRaWAN system of specifications (including the back-end, the Firmware Update Over The Air (FUOTA), etc.) becomes completely reusable, which represents a decisive strength for the commercial viability of GM. Of course, here LoRaWAN is just a specific (though certainly important) example, and the byte oriented transmission made possible by the use of a sequence length equal to a power of 2 opens the possibility to use GM in many other systems.

VII. CONCLUSION

In this paper, we introduced Golden Modulation, a novel modulation with ultra-long range capability and massive capacity. The basic modulation principles relying on spectrum spreading via direct Zadoff-Chu sequences modulation have been presented and the corresponding theoretical BER performance in AWGN channel has been derived and compared by simulation with realistic Golden Modulation receiver performance. A basic low complexity DFT-based receiver has been described. The fundamentals of multi-user operation have been studied and the corresponding multi-user interference evaluated from both a theoretical and a simulation point view. The very low multi-user interference level, even in uncoordinated conditions, coupled with the numerous available

waveforms, unlocks the well-known capacity bottleneck of IoT networks. In particular, while being equivalent to LoRa in a single-user setting, GM is vastly superior when it comes to multi-user performance. Overall, the low complexity receiver, flexible frame structure and minimal protocol constraints of GM pave the way for the deployment of LPWAN networks with truly massive capacity, or for the upgrade of existing ones. Furthermore, the possibility to use an effective sequence length equal to a power of 2 makes GM suitable as the physical layer for many existing protocol suites.

Future work includes a more detailed analytical characterization of the interference and multiple-access behavior of GM, as well as a thorough study of the performance of the entire system.

APPENDIX
CLOSED FORM EXPRESSION OF GOLDEN MODULATION BER

According to Equation (7), the discrete-time signal space for the Golden Modulation admits as an orthonormal basis the set of sequences $\frac{1}{\sqrt{N}} x(kT_c; q, N; r)$ indexed by the possible transmitted symbol $q \in \{0, 1, \dots, M-1\}$ and for the running time index $k \in \{0, 1, \dots, N-1\}$. Except for the notation, the detection problem is the same as in [27], where the bit error probability has been derived as

$$P_b = \int_0^\infty \left[1 - \left[1 - \exp\left[-\frac{\beta^2}{2\,\sigma^2} \right] \right]^{2^{SF-1}} \right] f_\beta(\beta)\,d\beta \quad (12)$$

where $\sigma^2 = \frac{N_0}{2}$, with N_0 the single-sided noise power spectral density, and $f_\beta(\beta)$ is the probability density function for the Rician distributed β with shape parameter $\kappa_\beta = \frac{E_S}{N_0} = \frac{SF}{N_0}$. Further noticing the very high spreading gains used and applying Gaussian approximations, [27] derives an approximation of the corresponding bit error probability valid for high spreading gains

$$P_b \approx 0.5\, Q(\sqrt{\Gamma.2^{SF+1}} - \sqrt{1.386.SF + 1.154}) \quad (13)$$

where Γ is the SNR. This expression is also valid for GM. Corroborating this statement, the simulations performed with $SF = 8, 12, 16$ show a very good match with the curves predicted by Equation (13), as shown in Fig. 2.

ACKNOWLEDGMENT

The authors would like to thank Prof. Fabien Ferrero from the University of Nice (UCA-LEAT) for the constructive discussions and for his support for the experimental validations of the Golden Modulation performed in his laboratory premises.

REFERENCES

[1] L. Vangelista, B. Jechoux, J. X. Canonici, and M. Zorzi, "The golden modulation for massive IoT," in *Proc. 21st Medit. Commun. Comput. Netw. Conf. (MedComNet)*, Jun. 2023, pp. 184–187.

[2] D. Zucchetto and A. Zanella, "Uncoordinated access schemes for the IoT: Approaches, regulations, and performance," *IEEE Commun. Mag.*, vol. 55, no. 9, pp. 48–54, Sep. 2017.

[3] Z. Gao, M. Ke, L. Qiao, and Y. Mei, *Massive IoT Access for 6G*. Singapore: Springer, 2022.

[4] M. Mohammadkarimi, O. A. Dobre, and M. Z. Win, "Massive uncoordinated multiple access for beyond 5G," *IEEE Trans. Wireless Commun.*, vol. 21, no. 5, pp. 2969–2986, May 2022.

[5] M. B. Hassan, A. E. Sayed, R. A. Mokhtar, R. A. Saeed, and B. S. Chaudhari, "NB-IoT: Concepts, applications, and deployment challenges," in *LPWAN Technologies for IoT and M2M Applications*. New York, NY, USA: Academic, 2020.

[6] P. Banelli, G. Colavolpe, L. Rugini, and A. Ugolini, "Waveform design," in *Information Theoretic Perspectives on 5G Systems and Beyond*, I. Maric, S. Shamai (Shitz), and O. Simeone, Eds. Cambridge, U.K.: Cambridge Univ. Press, 2022.

[7] I. Maric, S. Shamai (Shitz), and O. Simeone, *Information Theoretic Perspectives on 5G Systems and Beyond*. Cambridge, U.K.: Cambridge Univ. Press, 2022.

[8] R. Kovalchukov et al., "DECT-2020 new radio: The next step toward 5G massive machine-type communications," *IEEE Commun. Mag.*, vol. 60, no. 6, pp. 58–64, Jun. 2022.

[9] A. Lavric, A. I. Petrariu, and V. Popa, "Long range SigFox communication protocol scalability analysis under large-scale, high-density conditions," *IEEE Access*, vol. 7, pp. 35816–35825, 2019.

[10] L. Vangelista, "Frequency shift chirp modulation: The LoRa modulation," *IEEE Signal Process. Lett.*, vol. 24, no. 12, pp. 1818–1821, Dec. 2017.

[11] M. Chiani and A. Elzanaty, "On the LoRa modulation for IoT: Waveform properties and spectral analysis," *IEEE Internet Things J.*, vol. 6, no. 5, pp. 8463–8470, Oct. 2019.

[12] C. Pham, A. Bounceur, L. Clavier, U. Noreen, and M. Ehsan, "Radio channel access challenges in LoRa low-power wide-area networks," in *LPWAN Technologies for IoT and M2M Applications*. New York, NY, USA: Academic, 2020.

[13] M. Jouhari, N. Saeed, M.-S. Alouini, and E. M. Amhoud, "A survey on scalable LoRaWAN for massive IoT: Recent advances, potentials, and challenges," *IEEE Commun. Surveys Tuts.*, vol. 25, no. 3, pp. 1841–1876, 3rd Quart., 2023.

[14] F. Benkhelifa, Y. Bouazizi, and J. A. McCann, "How orthogonal is LoRa modulation?" *IEEE Internet Things J.*, vol. 9, no. 20, pp. 19928–19944, Oct. 2022.

[15] (2018). *TS001-1.0.4 LoRaWAN L2 1.0.4 Specification*. [Online]. Available: https://resources.lora-alliance.org/technical-specifications/lorawan-specification-v1-0-3

[16] A. Kadambi and R. Kadlimatti, "Doppler tolerant and detection capable polyphase good code sets based on linear FM waveforms," in *Proc. 19th Eur. Radar Conf. (EuRAD)*, Sep. 2022, pp. 1–4.

[17] D. Chu, "Polyphase codes with good periodic correlation properties (Corresp.)," *IEEE Trans. Inf. Theory*, vol. IT-18, no. 4, pp. 531–532, Jul. 1972.

[18] M. Hyder and K. Mahata, "Zadoff–Chu sequence design for random access initial uplink synchronization in LTE-like systems," *IEEE Trans. Wireless Commun.*, vol. 16, no. 1, pp. 503–511, Jan. 2017.

[19] Z. Zhang, R. Rathi, S. Perez, J. Bukhari, and Y. Zhong, "ZCNET: Achieving high capacity in low power wide area networks," *IEEE/ACM Trans. Netw.*, vol. 30, no. 5, pp. 2032–2045, Oct. 2022.

[20] C. Bernier, F. Dehmas, and N. Deparis, "Low complexity LoRa frame synchronization for ultra-low power software-defined radios," *IEEE Trans. Commun.*, vol. 68, no. 5, pp. 3140–3152, May 2020.

[21] L. Vangelista and A. Cattapan, "Start of packet detection and synchronization for LoRaWAN modulated signals," *IEEE Trans. Wireless Commun.*, vol. 21, no. 6, pp. 4608–4621, Jun. 2022.

[22] M. Centenaro, C. E. Costa, F. Granelli, C. Sacchi, and L. Vangelista, "A survey on technologies, standards and open challenges in satellite IoT," *IEEE Commun. Surveys Tuts.*, vol. 23, no. 3, pp. 1693–1720, 3rd Quart., 2021.

[23] D. Wang, A. Traspadini, M. Giordani, M.-S. Alouini, and M. Zorzi, "On the performance of non-terrestrial networks to support the Internet of Things," in *Proc. 56th Asilomar Conf. Signals, Syst., Comput.*, Oct. 2022, pp. 881–887.

[24] R. Marini, K. Mikhaylov, G. Pasolini, and C. Buratti, "Low-power wide-area networks: Comparison of LoRaWAN and NB-IoT performance," *IEEE Internet Things J.*, vol. 9, no. 21, pp. 21051–21063, Nov. 2022.

[25] D. Yang et al., "Understanding power consumption of NB-IoT in the wild: Tool and large-scale measurement," in *Proc. 26th Annu. Int. Conf. Mobile Comput. Netw.*, Sep. 2020, pp. 1–13.

[26] B. M. Popovic, "Generalized chirp-like polyphase sequences with optimum correlation properties," *IEEE Trans. Inf. Theory*, vol. 38, no. 4, pp. 1406–1409, Jul. 1992.

[27] T. Elshabrawy and J. Robert, "Closed-form approximation of LoRa modulation BER performance," *IEEE Commun. Lett.*, vol. 22, no. 9, pp. 1778–1781, Sep. 2018.

[28] J. Petajajarvi, K. Mikhaylov, A. Roivainen, T. Hanninen, and M. Pettissalo, "On the coverage of LPWANs: Range evaluation and channel attenuation model for LoRa technology," in *Proc. 14th Int. Conf. ITS Telecommun. (ITST)*, Dec. 2015, pp. 55–59.

[29] J. Petäjäjärvi, K. Mikhaylov, M. Pettissalo, J. Janhunen, and J. Iinatti, "Performance of a low-power wide-area network based on LoRa technology: Doppler robustness, scalability, and coverage," *Int. J. Distrib. Sensor Netw.*, vol. 13, no. 3, Mar. 2017, Art. no. 155014771769941, doi: 10.1177/1550147717699412.

[30] H. Linka, M. Rademacher, O. G. Aliu, and K. Jonas, *Path Loss Models for Low-Power Wide-Area Networks: Experimental Results Using LoRa*. Berlin, Germany: VDE Verlag, 2018.

[31] ETSI, *Short Range Devices (SRD) Operating in the Frequency Range 25 MHz to 1 000 MHz; Part 1: Technical Characteristics and Methods of Measurement*, European Telecommunication Standardization Institute, European Norm (EN) ETSI EN 300 220-1, Sophia Antipolis, France, Version 3.1.1, Feb. 2017. [Online]. Available: https://www.etsi.org/deliver/etsi_en/300200_300299/30022001/03.01.01_60/en_30022001v030101p.pdf

[32] M. Frigo and S. G. Johnson. *Fastest Fourier Transform in the West*. Accessed: Jul. 28, 2022. [Online]. Available: http://www.fftw.org/

[33] L. Welch, "Lower bounds on the maximum cross correlation of signals (Corresp.)," *IEEE Trans. Inf. Theory*, vol. IT-20, no. 3, pp. 397–399, May 1974.

[34] M. Antweiler, "Merit factor of Chu and Frank sequences," *Electron. Lett.*, vol. 26, no. 25, pp. 2068–2070, Dec. 1990.

[35] W. H. Mow and S.-Y.-R. Li, "Aperiodic autocorrelation properties of perfect polyphase sequences," in *Proc. ICCS/ISITA*, Singapore, 1992, pp. 1232–1234.

[36] P. Z. Fan, M. Darnell, and B. Honary, "Polyphase sequences with good periodic and aperiodic autocorrelations," in *Proc. IEEE Int. Symp. Inf. Theory*, Jun. 1994, p. 74.

[37] W. Ho Mow and S.-Y.-R. Li, "Aperiodic autocorrelation and crosscorrelation of polyphase sequences," *IEEE Trans. Inf. Theory*, vol. 43, no. 3, pp. 1000–1007, May 1997.

[38] A. Zanella and M. Zorzi, "Theoretical analysis of the capture probability in wireless systems with multiple packet reception capabilities," *IEEE Trans. Commun.*, vol. 60, no. 4, pp. 1058–1071, Apr. 2012.

[39] M. O. Shahid, M. Philipose, K. Chintalapudi, S. Banerjee, and B. Krishnaswamy, "Concurrent interference cancellation: Decoding multi-packet collisions in LoRa," in *Proc. ACM SIGCOMM Conf.* New York, NY, USA: Association for Computing Machinery, Aug. 2021, pp. 503–515, doi: 10.1145/3452296.3472931.

[40] (2022). *RP002-1.0.4 Regional Parameters*. [Online]. Available: https://resources.lora-alliance.org/technical-specifications/rp002-1-0-4-regional-parameters

[41] B. S. Chaudhari and M. Zennaro, *LPWAN Technologies for IoT and M2M Applications*. Amsterdam, The Netherlands: Elsevier, 2020.

Bruno Jechoux received the M.Sc. degree in electrical engineering from Centrale-Supelec Engineering School in 1994, with a specialization in radio-communications. He has more than 20 years of experience in the design and standardization of advanced wireless systems, including WiFi, LTE, and 5G. Prior to co-founding Ternwaves, he has been with Mitsubishi, Motorola, Infineon, Intel, and TCL. From 2011 to 2016, he was with Intel, where he was a Principal Wireless System Engineer in charge of defining the 4G and 4.5G modems architecture. From 2016 to 2021, he was the Head of the TCL 5G European Research Laboratory (Sophia Antipolis, France) in charge of 5G standardization and advanced 5G demonstrator (world's first 5G full software implementation at Mobile World Congress 2018). He is currently the author of more than 50 patents.

Jean-Xavier Canonici received the M.Sc. degree in electrical engineering from Centrale-Supelec Engineering School in 1994, with a specialization in digital communications and electronics. He has 25 years of experience in modem definition and development for fixed wireless, satellite, cellular 3G/4G, and 5G-IoT. His experience was built in the following companies: Intel Mobile Communications, Sequans, Infineon, Siemens, Alcatel Telspace, Alcatel CIT, and CEA. From 2011 to 2016, he was with Intel, as a Principal Engineer of wireless systems. He was the Head of the Modem System Engineering Team, working more specifically on high-end smartphone platforms for lead customers, such as Apple or Samsung. He was just before the creation of a Ternwaves Principal Physical Layer Algorithms and Technical Manager with Sequans in charge of NB-IoT modem for CatM1/CatNB1 platforms. He holds more than ten U.S. patents.

Michele Zorzi (Fellow, IEEE) received the Laurea and Ph.D. degrees in electrical engineering from the University of Padova, Padua, Italy, in 1990 and 1994, respectively. From 1992 to 1993, he was on leave with the University of California at San Diego (UCSD), USA. In 1993, he joined the Faculty of Dipartimento di Elettronica, Informazione e Bioingegneria, Politecnico di Milano, Milan, Italy. After spending three years with the Center for Wireless Communications, UCSD. In 1998, he joined the School of Engineering, University of Ferrara, Ferrara, Italy, where he was a Professor in 2000. Since November 2003, he has been with the Department of Information Engineering, University of Padova. His current research interests include performance evaluation in mobile communications systems, wireless sensor networks, the Internet of Things, cognitive communications and networking, millimeter-wave and terahertz communications, vehicular networks, non-terrestrial networks, and underwater communications and networks. He has served as the Member-at-Large for the Board of Governors of the IEEE Communications Society from 2009 to 2011 and from 2021 to 2023. He received several awards from the IEEE Communications Society, including the Best Tutorial Paper Award in 2008 and 2019, the Education Award in 2016, the Stephen O. Rice Best Paper Award in 2018, and the Joseph LoCicero Award for Exemplary Service to Publications in 2020. He was the Editor-in-Chief of *IEEE Wireless Communications Magazine* from 2003 to 2005, IEEE TRANSACTIONS ON COMMUNICATIONS from 2008 to 2011, and IEEE TRANSACTIONS ON COGNITIVE COMMUNICATIONS AND NETWORKING from 2014 to 2018. He was the Director of Education from 2014 to 2015 and the Director of Journals from 2020 to 2021.

Lorenzo Vangelista (Senior Member, IEEE) received the Laurea and Ph.D. degrees in electrical and telecommunication engineering from the University of Padova, Padua, Italy, in 1992 and 1995, respectively. He subsequently joined the Transmission and Optical Technology Department, CSELT, Turin, Italy. From December 1996 to January 2002, he was with Telit Mobile Terminals, Trieste, Italy. In May 2003, he was with Microcell A/S, Copenhagen, Denmark. In July 2006, he joined the Worldwide Organization, Infineon Technologies, as a Program Manager. From October 2006 to October 2021, he was an Associate Professor of telecommunication with the Department of Information Engineering, University of Padova, where he is currently a Full Professor. His research interests include signal theory, multicarrier modulation techniques, cellular networks, and the Internet of Things connectivity with a special focus on low power wide area networks.